Direct Magnetization-Polarization Coupling in $BaCuF_4$

A. C. Garcia-Castro,[1,2,*] W. Ibarra-Hernandez,[3,4] Eric Bousquet,[2] and Aldo H. Romero[3,4,†]
[1]*Department of Physics, Universidad Industrial de Santander, Carrera 27 Calle 9, Bucaramanga, Colombia*
[2]*Physique Théorique des Matériaux, CESAM, Université de Liège, B-4000 Sart-Tilman, Belgium*
[3]*Department of Physics and Astronomy, West Virginia University, Morgantown, West Virginia WV-26506-6315, USA*
[4]*Facultad de Ingeniería-BUAP, Apartado Postal J-39, Puebla, Pue. 72570, Mexico*

(Received 2 April 2018; revised manuscript received 4 August 2018; published 11 September 2018)

Herewith, first-principles calculations based on density functional theory are used to describe the ideal magnetization reversal through polarization switching in $BaCuF_4$ which, according to our results, could be accomplished close to room temperature. We also show that this ideal coupling is driven by a single soft mode that combines both polarization, and octahedral rotation. The later being directly coupled to the weak ferromagnetism of $BaCuF_4$. This, added to its strong Jahn-Teller distortion and its orbital ordering, makes this material a very appealing prototype for crystals in the ABX_4 family for multifunctional applications. The described mechanism behaves ideally as it couples the ferroelectric and the magnetic properties naturally and it has not been reported previously.

DOI: 10.1103/PhysRevLett.121.117601

The search for materials that own ferroelectricity, magnetization, and orbital ordering with a large coupling between those properties, has become one of the most active research fields in condensed matter physics. Over the last decade, it has received vigorous interest by many different research groups due to their high potential in new technologies where multifunctionalities are required. Among these couplings, magnetoelectricity promises to reduce computer memory energy consumption, to improve magnetic field sensors and/or to be used for spintronic applications [1]. Magnetoelectric crystals, however, suffer from their scarcity, their small response, and their low functioning temperature. In spite of the great improvements in identifying and understanding the underneath mechanism of magnetoelectricity, finding new room-temperature candidates has been difficult and their number is quite scarce. One of possible solutions is to create those materials as composites, but magnetoelectric single crystals are still very rare at the present stage of knowledge in this research field [1]. Another proposed solution to find good magnetoelectric single crystals has been to identify new ferroelectric materials, where the ferroelectric (FE) ordering can be coupled to the magnetization [2,3]. To that end, novel stoichiometries and compositions have been investigated and a promising approach is to look for layered perovskite materials where the octahedra rotations are linked to the polarization through improperlike couplings [2–5]. Indeed, Ruddlesden-Popper, Aurivillius, and Dion-Jacobson [4] phases have been shown to be good candidates to exhibit such coupling between polarization and magnetism. The proof of concept has been shown theoretically by Benedek and Fennie in $Ca_3Mn_2O_7$ [2], where the coupling mechanism with magnetism relies on the improper origin of the polarization that indirectly couples with the magnetization. Unfortunately, the experimental efforts to verify this prediction have, so far, shown that the electric polarization in $Ca_3Mn_2O_7$ cannot be switched, which seems to indicate that this crystal might not be the best candidate for magnetization reversal through an electric field [6]. Moreover, in practice, complex switching paths, where rotations are combined so that it prevents the polarization reversal, are now becoming accessible in materials, where the coupling is based on the hybrid-improper mechanism [6]. Following the same strategy, layered materials with formula $A_nB_nX_{3n+2}$ appeared to be other favorable candidates [7–9]. In these crystal types, the octahedral rotations and the polar distortions are intrinsically coupled in a single mode through improperlike couplings as in the previous case [10]. However, here again, while the proof of concept has been shown, a specific material candidate is still missing.

In this Letter, we show from first-principles calculations (computational details are in the Supplemental Material [11], which includes Refs. [12–25]) that within the family of the barium-based layered fluorides $BaMF_4$ [26,27], the case of $BaCuF_4$ has an ideal direct coupling between polarization and magnetization that does not rely on an improper mechanism. Unlike previous reported mechanisms, the ferromagnetic coupling involves here a single phonon mode, where changes in the polarization drives naturally changes in the magnetization. Combined with the rather high Néel temperature $T_N = 275$ K (the largest over $M = $ Mn, Ni, Co, and Fe series), this makes $BaCuF_4$ an appealing new candidate for electric-field-tuned magnetization. We also show that the peculiar coupling is linked to the subtle interplay between ferroelectricity, magnetism, and the Jahn-Teller (JT) effect.

In what follows, we start by describing the characterization of the ferroic orders in this compound, such that we can understand the correlation between the ferroelectricity and the weak-ferromagnetic state of $\mathrm{BaCuF_4}$.

Ferroelectric ordering.—The Ba$M$$\mathrm{F_4}$ family of compounds is structurally characterized by octahedral $M\mathrm{F_6}$ layers separated by Ba sheets stacked along the y axis as shown in Fig. 1. We start by analyzing the phonon modes of the hypothetical high-symmetry structure of $\mathrm{BaCuF_4}$ fluoride ($Cmcm$ space group, No. 63), not observed experimentally before the melting temperature (around 1000 K) [28]. The computed phonon dispersion of the high-symmetry reference (Fig. S1 in the Supplemental Material [11]) reveals the presence of three unstable phonon modes, when looking at the zone center and zone boundary points: Γ_2^- at 66, S_2^+ at 57, and Y_2^- at 47 $i\mathrm{cm}^{-1}$.

The Γ_2^- mode is polar and combines polar motion of the Ba atoms along the z direction with in-phase fluorine octahedra rotation around the x direction [see Fig. 1(a)] and its condensation reduces the symmetry of the crystal to the $Cmc2_1$ (No. 36) space group. The full relaxation of the crystal within the $Cmc2_1$ lowers the energy with respect to the $Cmcm$ phase by $\Delta E = -27$ meV per formula unit (meV/f.u.) and by decomposing the final distortions into symmetry adapted mode [29,30] we find a contribution of the $Cmcm$ Γ_1^+ and Γ_2^- mode. The Γ_1^+ mode is the mode that is invariant under all the symmetry operations of the $Cmcm$ phase, which means that it is a relaxation of the initial $Cmcm$ degrees of freedom that favors the development of the polarization. A similar combination of modes has been reported in the ferroelectric $\mathrm{LaTaO_4}$ [31] and $\mathrm{La_2Ti_2O_7}$ [10].

The S_2^+ mode drives the system to a nonpolar phase with $P2_1/c$ space group (No. 14) and its eigenvector is an out-of-phase octahedra rotation around the x axis (see Fig. S1 in the Supplemental Material [11]). We note that it is the same type of distortion as for the Γ_2^+ mode (i.e., octahedral rotation around the x axis) but in the case of the S_2^+ mode, the out-of-phase octahedral rotations do not break the space inversion symmetry. The gain of energy due to the relaxation of the $P2_1/c$ phase is $\Delta E = -7$ meV/f.u., thus about 4 times smaller than the $Cmc2_1$ phase.

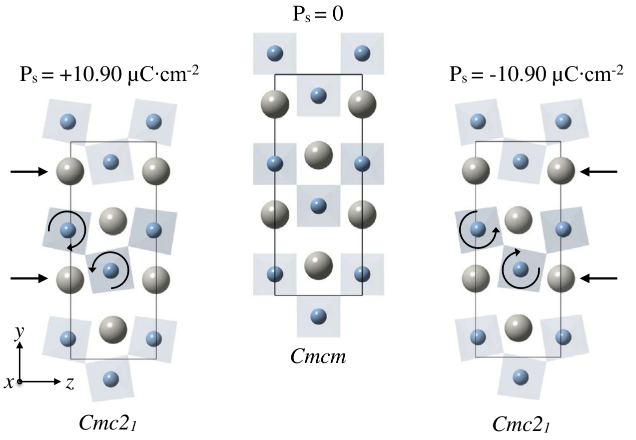

FIG. 1. $Cmcm$ and $Cmc2_1$ phases of the $\mathrm{BaCuF_4}$. The phase transition responsible for the ferroelectric switching involves the octahedral (in blue with Cu at the center) rotations around the x axis as well as the polar Ba sites (in dark gray). The later rotations and displacements, denoted with arrows, belong to the Γ_2^- mode.

The condensation of the Y_2^- mode reduces the symmetry of the crystal into the $Pnma$ space group (No. 62) where its eigenvector involves in-phase clockwise rotation of the octahedra around the x axis in one octahedral layer and an in-phase counterclockwise in the next octahedral layer (as shown in Fig. S1 in the Supplemental Material [11]). The relaxation of the $Pnma$ phase lowers the energy by $\Delta E = -10$ meV/f.u., which is larger than the $P2_1/c$ phase but more than 2 times smaller than the $Cmc2_1$ phase.

We thus find that the ferroelectric $Cmc2_1$ phase is the ground state of $\mathrm{BaCuF_4}$, which agrees with experiments [32,33]. The phonon dispersion shows its local stability as there is not imaginary frequencies in the full Brillouin zone (Fig. S1 in Supplemental Material [11]). In this compound, in contrast to the other members of the same Ba$M$$\mathrm{F_4}$ family, we note a strong JT distortion. The latter is caused by Cu:d^9 orbital filling, which is also present in the high-symmetry $Cmcm$ structure and induces a large octahedra elongation along the x axis. Therefore, we found that the Cu-F bonding distances in the $Cmc2_1$ phase are 2.25, 1.88, and 1.91 Å for the bonds along the [1,0,0], [0,1,1], and [0, −1, −1] directions, respectively. The relaxed a, b, and c lattice parameters are 4.453, 13.892, and 5.502 Å, respectively, which are close to the experimental values of 4.476, 13.972, and 5.551 Å [32,33]. Thus, when comparing with other members of the family, the Cu-F bonding length, along the x axis, is by far the largest with an elongation close to 0.2 Å. The later elongation (induced by the strong JT effect as a response of the electronic Cu:d^9 configuration) has strong effects into the magnetic structure, which will be discussed later.

The computed polarization in the ground state is $P_s = 10.9\ \mu\mathrm{C\,cm^{-2}}$, being in the range of amplitudes of Ba$M$$\mathrm{F_4}$ compounds (see Table I). The computed energy difference between the $Cmcm$ and the $Cmc2_1$, is $\Delta E = 27$ meV/f.u., which is lower than the one reported for other family members such as $\mathrm{BaMgF_4}$ and $\mathrm{BaZnF_4}$ with barriers of 133 and 218 meV/f.u. but similar to $\mathrm{BaNiF_4}$ and $\mathrm{BaCoF_4}$ where the ferroelectric switching has been experimentally demonstrated [26]. This low barrier value suggests that the ferroelectric switching can be easier. In order to estimate how the polarization of $\mathrm{BaCuF_4}$ fits with respect to the members of the Ba$M$$\mathrm{F_4}$ family, in Table I we compare the trend of the polarization's amplitude as a function of the M^{2+} ionic radii [34]. We observe that the polarization follows the trend of the ionic radii size, which is expected from geometrically driven polar displacements [35], also concluded from their close-to-nominal Born

TABLE I. Polarization and ionic M^{2+} radii [34] for all the members of the Ba*M*F$_4$ family. A clear trend of the polarization dependent of the octahedral cation size is observed in full agreement with the geometric proper ferroelectricity observed in these fluoride compounds. No experimental ferroelectric switching has been demonstrated for BaMnF$_4$ and BaFeF$_4$. Finally, in the last column, the energy barrier values for all considered compounds taken from the *Cmcm* to the *Cmc*2$_1$ are presented.

Compound	M^{2+} radii [pm]	P$_s$ [μC cm^{-2}]	ΔE [meV/f.u.]
BaNiF$_4$	83	6.8 [38]	28 [38]
BaMgF$_4$	86	9.9	133 [39]
BaCuF$_4$	87	10.9	27
BaZnF$_4$	88	12.2	218 [39]
BaCoF$_4$	88.5	9.0 [38]	58 [38]
BaFeF$_4$	92	10.9 [38]	122 [38]
BaMnF$_4$	97	13.6 [38]	191 [38]

effective charges (see Supplemental Material [11]) similarly as theoretically predicted [36] and later experimentally demonstrated in the multiferroic NaMnF$_3$ perovskite fluoride [37]. Interestingly, it can be also noted that BaMnF$_4$ and BaFeF$_4$, which lack experimentally proved polarization reversal [26], are those with the largest M^{2+} ionic radii. The latter suggests a delicate balance between geometric effects and the switching process that needs to be further investigated.

Magnetic ordering: The analysis of the possible main collinear magnetic orderings of BaCuF$_4$ reveals the existence of an 1D-AFM thanks to its strong JT distortion. This ordering is confirmed by the calculated magnetic exchange constants (computed following the procedure of Ref. [40]) where values of 0.04, 0.03, and −15.91 meV were obtained for J_a, J_b, and J_c, respectively [see notation in Fig. 2(a)]. We find that J_a and J_b are very small, which explains the 1D-AFM character at high temperatures. Moreover, the spin-polarized charge density [see Fig. 2(b)], clearly shows the ferrodistortive character of the $d_{x^2-y^2}$ orbital ordering thanks to the strong JT distortion present in this Cu: d^9 compound and then, leading as a result to the 1D-AFM character. More details about the magnetic orderings can be found in the Supplemental Material [11], including Refs. [32,40,41], and we would like to focus on the noncollinear magnetism analysis next.

Starting from the 1D AFM (also known as *A*-AFM) in the noncollinear magnetic ordering regime, we observe the appearance of spin canting giving a weak-ferromagnetic (*w*-FM) moment along the *z* axis, with $m_z = 0.059\,\mu_B/\text{atom}$. The system can be described by the modified Bertaud's notation [42,43] as A_yF_z where the *A*-AFM is the main ordering along the *y* axis ($m_y = 0.829\ \mu_B/\text{atom}$) and canted ferromagnetism F_z along the *z* direction. We thus obtain a magnetic canting angle of about 4.12° with respect to the *y* axis. Although, a noncollinear ordering has been observed for $M =$ Mn, Fe, Co, and Ni too, the canted structure gives rise to a weak-AFM ordering instead [38,44], as shown in the Supplemental Material [11]. Then, our findings in Cu case confirm that both the spontaneous polarization and the ferromagnetic moment are conveniently aligned along the *c* axis. Interestingly, this canting angle is larger than those reported for the weak-AFM $M =$ Ni [44] and Ca$_3$Mn$_3$O$_7$ [2]. Besides, even when the magnetic measurements [32] show that above 275 K the material exhibits a paramagnetic behavior, the JT distortion is expected to remain in the structure due to a survival of the orbital ordering beyond T_N as we observed in the relaxed *Cmcm*. This has a direct effect on the octahedral structure as observed for KCuF$_3$ [45].

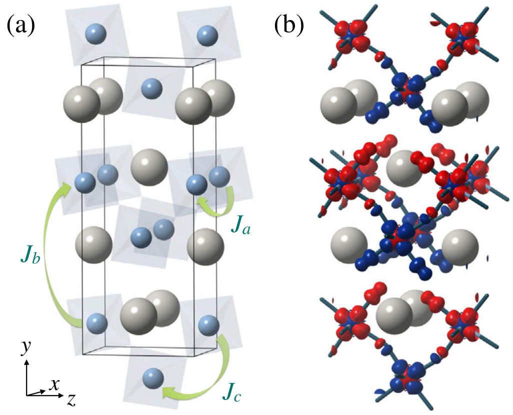

FIG. 2. (a) *Cmc*2$_1$ structure where the magnetic exchange constants of the intralayer J_a and J_c and the interlayer J_b constant are depicted. (b) Spin-polarized charge density, where a clear orbital ordering, induced by the strong JT distortion, is observed. Here, the magnetic moment up and down are depicted in red and blue, respectively.

Intertwined magnetization and polarization.—Through the presence of both magnetization and polarization one can see that BaCuF$_4$ can hold up to 4 multiferroic states (i.e., M^-P^+, M^-P^-, M^+P^+, and M^+P^-) as shown in Fig. 3(a). In the following, we are going to show that the magnetization can be switched by means of an applied electric field, thanks to the spontaneous polarization reversal, and by the AFM-domain reversal thanks to its canted structure.

We performed the computed experiment where the full ground state distortion is gradually frozen into the *Cmcm* reference phase. At each point the electronic structure is relaxed (and thus the noncollinear magnetization) with fixed geometry. In Figs. 3(b) and 3(c) we show the energy well and the associated polarization at different distortion amplitudes respectively. The ferroelectric polarization shows a full reversal from −10.9 to +10.9 μC cm^{-2} as well as the octahedral rotation angle, taking as a reference the Cu-F-Cu bonding in the *Cmcm* structure. The spin (m_z) and orbital (l_z) moments, plotted in Fig. 3(d), show that $m_z \gg l_z$, and most importantly that the magnetization, changes its sign when the polarization is reversed. In order

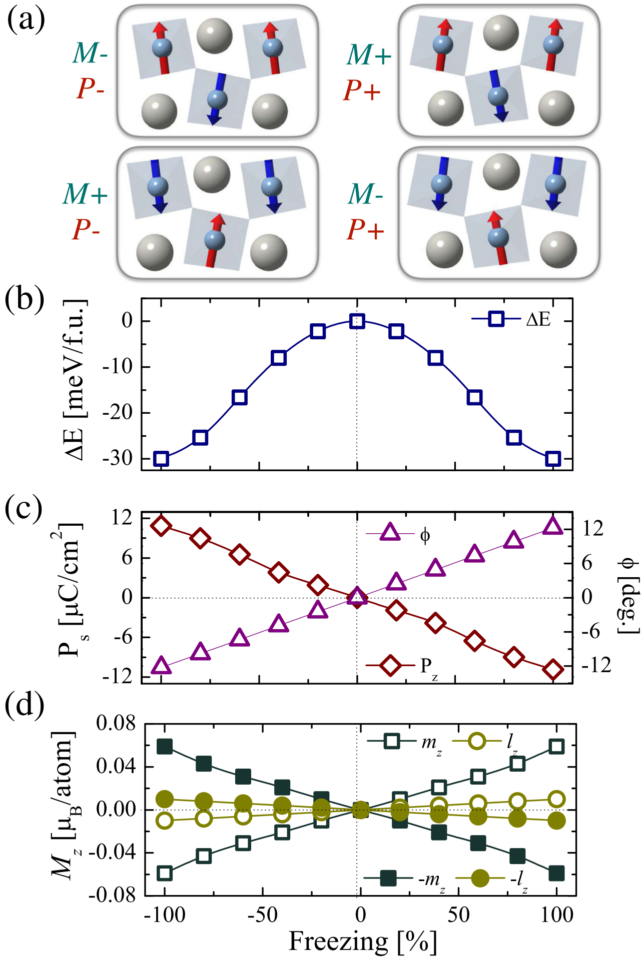

FIG. 3. (a) Schematic representation of the four multiferroic states where the ferroelectric polarization and magnetization are shown in $BaCuF_4$. Here, only one of the octahedral layers is shown, the others keep the same octahedral pattern and magnetic ordering. It can be observed that the magnetic moments, depicted as red and blue arrows for up and down orientation, respectively, can be reversed by switching the magnetic ordering and/or the polarization reversal. (b) Double-well energy profile obtained through the ferroelectric switching between the up and down spontaneous polarization orientations. (c) Full polarization reversal going from -10.9 to $+10.9\ \mu\mathrm{C\,cm^{-2}}$ as well as the octahedral rotation angle ϕ, where a full octahedral reversal is observed. (d) Magnetic (m_z) and orbital (l_z) moments reversal by means of the ferroelectric switching showing the correlation between the switching, rotations, and noncollinear magnetic ordering. Solid and open symbols represent the magnetic moments for P_s up and down orientation, respectively.

to obtain the w-FM component switching when the polarization is clamped, the AFM-domain reversal is required. Fortunately, the later process has been demonstrated to be feasible for other systems, where, electrically controlled multifunctional applications have been achieved [46,47]. Therefore, as expected the four multiferroic states are possible, and more importantly, their magnetization and polarization directions could be reversed in this type of material. Additionally, the magnetoelectric coupling via polarization tuning by means of an applied magnetic field also show a response as commented on in the Supplemental Material [11], which includes Ref. [48].

This link between the polarization and the magnetization can be explained in terms of the Dzyaloshinskii-Moriya (DM) interaction [49,50] that is related to the rotation of the octahedra. The DM interaction energy is defined by the relationship $E = \mathbf{D}_{ij} \cdot (s_i \times s_j)$, where $\mathbf{D}_{ij}$ is the DM tensor and the s_i and s_j are the spins related to the ions i and j, respectively. As demonstrated in perovskites [51], the DM tensor can be related to the interionic vectors as $\mathbf{D}_{ij} \propto (\hat{x}_i \times \hat{x}_j)$ [51], where $\hat{x}_i$ and $\hat{x}_j$ are unitary vectors along the Cu-F-Cu bonds. In $BaCuF_4$, the absence of octahedral rotation in the high-symmetry *Cmcm* structure gives a 180° Cu-F-Cu bonding angle and thus forbids a w-FM ordering. A key feature in this type of system is that the polarization and octahedra rotations are embedded into the same unstable mode of the *Cmcm* structure such that reversing the polarization will systematically reverse the octahedral rotation and thus the w-FM. The later in contrast to hybrid-improper based materials where the reversal of two rotations can leave the polarization unchanged [6]. It is important to mention that the noncollinear ordering is also observed in all of the other magnetic phases (G-AFM and C-AFM) but never with a w-FM moment. Thus, $BaCuF_4$ ideally combines the desired magnetic ordering, thanks to the JT distortion, with the appropriated structural ground state over the AMF_4 family to exhibit a perfect electric-field magnetization reversal. It has thus a large magnetoelectric effect at rather large temperature and can be used to build a four-states memory device as discussed before.

Although at first glance the magnetic moment could be seen to be weak, it could be amplified by layer engineering and growing a ferromagnetic layer on the top of it as demonstrated through the exchange-bias effect [52] in $[\mathrm{Co/Pd(Pt)}]/\mathrm{Cr_2O_3}$ [53] and NiFe/h-$YMnO_3$ ($LuMnO_3$) [54] but also in the barium-based family of AMF_4 crystals with $M =$ Ni and Mn [55,56]. Therefore, the bilayered exchange-bias effect could be combined to bring about a novel electrically controlled magnetic system based on $BaCuF_4$ [52]. In conclusion, we believe the $BaCuF_4$ compound is an ideal candidate to show a strong multiferroic-magnetoelectric coupling close to room temperature, being, to our knowledge, the only fluoride material that exhibits such behavior close to room temperature [57].

This work used the XSEDE, which is supported by National Science Foundation Grant No. ACI-1053575. A. C. G. C. and E. B. acknowledge the ARC project AIMED and the F. R.S-FNRS PDR project MaRePeThe. The authors also acknowledge the support from the Texas Advances Computer Center (with the Stampede2 and Bridges supercomputers), the PRACE project TheDeNoMo and on the CECI facilities funded by

F. R.S-FNRS (Grant No. 2.5020.1) and Tier-1 supercomputer of the Fédération Wallonie-Bruxelles funded by the Walloon Region (Grant No. 1117545). This work was supported by the DMREF-NSF 1434897, NSF OAC-1740111, and DOE DE-SC0016176 projects.

---

[*] a.c.garcia.castro@gmail.com
[†] alromero@mail.wvu.edu

[1] M. Fiebig, Nat. Rev. Mater. **1**, 16046 (2016).
[2] N. A. Benedek and C. J. Fennie, Phys. Rev. Lett. **106**, 107204 (2011).
[3] E. Bousquet, M. Dawber, N. Stucki, C. Lichtensteiger, P. Hermet, S. Gariglio, J.-M. Triscone, and P. Ghosez, Nature (London) **452**, 732 (2008).
[4] N. A. Benedek, J. M. Rondinelli, H. Djani, P. Ghosez, and P. Lightfoot, Dalton Trans. **44**, 10543 (2015).
[5] J. Young, A. Stroppa, S. Picozzi, and J. M. Rondinelli, J. Phys. Condens. Matter **27**, 283202 (2015).
[6] B. Gao, F.-T. Huang, Y. Wang, J.-W. Kim, L. Wang, S.-J. Lim, and S.-W. Cheong, Appl. Phys. Lett. **110**, 222906 (2017).
[7] M. Scarrozza, M. B. Maccioni, G. M. Lopez, and V. Fiorentini, Phase Transitions **88**, 953 (2015).
[8] M. Scarrozza, A. Filippetti, and V. Fiorentini, Phys. Rev. Lett. **109**, 217202 (2012).
[9] M. Scarrozza, A. Filippetti, and V. Fiorentini, Eur. Phys. J. B **86**, 128 (2013).
[10] J. López-Pérez and J. Íñiguez, Phys. Rev. B **84**, 075121 (2011).
[11] See Supplemental Material at http://link.aps.org/supplemental/10.1103/PhysRevLett.121.117601 for the information on the computational details, BaCuF4 phases condensation and phonon-dispersions, expanded magnetic ordering description, computed Born effective charges and obtained magnetoelectric coefficient. All the latter supporting the present manuscript.
[12] P. Hohenberg and W. Kohn, Phys. Rev. **136**, B864 (1964).
[13] W. Kohn and L. J. Sham, Phys. Rev. **140**, A1133 (1965).
[14] G. Kresse and J. Furthmüller, Phys. Rev. B **54**, 11169 (1996).
[15] G. Kresse and D. Joubert, Phys. Rev. B **59**, 1758 (1999).
[16] P. E. Blöchl, Phys. Rev. B **50**, 17953 (1994).
[17] J. P. Perdew, A. Ruzsinszky, G. I. Csonka, O. A. Vydrov, G. E. Scuseria, L. A. Constantin, X. Zhou, and K. Burke, Phys. Rev. Lett. **100**, 136406 (2008).
[18] A. I. Liechtenstein, V. I. Anisimov, and J. Zaanen, Phys. Rev. B **52**, R5467 (1995).
[19] J. Heyd, G. E. Scuseria, and M. Ernzerhof, J. Chem. Phys. **118**, 8207 (2003).
[20] A. V. Krukau, O. A. Vydrov, A. F. Izmaylov, and G. E. Scuseria, J. Chem. Phys. **125**, 224106 (2006).
[21] D. Legut and U. D. Wdowik, J. Phys. Condensed Matter **25**, 115404 (2013).
[22] D. Hobbs, G. Kresse, and J. Hafner, Phys. Rev. B **62**, 11556 (2000).
[23] X. Gonze and C. Lee, Phys. Rev. B **55**, 10355 (1997).
[24] K. Momma and F. Izumi, J. Appl. Crystallogr. **44**, 1272 (2011).
[25] D. Vanderbilt, J. Phys. Chem. Solids **61**, 147 (2000).
[26] M. Eibschütz, H. Guggenheim, S. Wemple, I. Camlibel, and M. DiDomenico, Phys. Lett. A **29**, 409 (1969).
[27] H. J. Monkhorst and J. D. Pack, Phys. Rev. B **13**, 5188 (1976).
[28] M. DiDomenico, M. Eibschütz., H. Guggenheim., and I. Camlibel, Solid State Commun. **7**, 1119 (1969).
[29] D. Orobengoa, C. Capillas, M. I. Aroyo, and J. M. Perez-Mato, J. Appl. Crystallogr. **42**, 820 (2009).
[30] J. M. Perez-Mato, D. Orobengoa, and M. I. Aroyo, Acta Crystallogr. Sect. A **66**, 558 (2010).
[31] X. Q. Liu, G. J. Li, and X. M. Chen, Solid State Commun. **247**, 31 (2016).
[32] J.-M. Dance, Mater. Res. Bull. **16**, 599 (1981).
[33] D. Babel and A. Tressaud, in *Inorganic Solid Fluorides*, edited by P. Hagenmuller (Academic Press, New York, 1985), p. 77.
[34] R. Shannon, Acta Crystallogr. Sect. A **A32**, 751 (1976).
[35] A. C. Garcia-Castro, N. A. Spaldin, A. H. Romero, and E. Bousquet, Phys. Rev. B **89**, 104107 (2014).
[36] A. C. Garcia-Castro, A. H. Romero, and E. Bousquet, Phys. Rev. Lett. **116**, 117202 (2016).
[37] M. Yang, A. KC, A. C. Garcia-Castro, P. Borisov, E. Bousquet, D. Lederman, A. H. Romero, and C. Cen, Sci. Rep. **7**, 7182 (2017).
[38] C. Ederer and N. A. Spaldin, Phys. Rev. B **74**, 024102 (2006).
[39] M. N. Valdez, H. T. Spanke, and N. A. Spaldin, Phys. Rev. B **93**, 064112 (2016).
[40] A. C. Garcia-Castro, A. H. Romero, and E. Bousquet, Phys. Status Solidi B **252**, 689 (2015).
[41] D. M. Korotin, V. V. Mazurenko, V. I. Anisimov, and S. V. Streltsov, Phys. Rev. B **91**, 224405 (2015).
[42] E. F. Bertaut, *Magnetism*, edited by G. T. Rado and H. Suhl (Academic Press, New York, 1963), Vol. 3.
[43] E. Bousquet and A. Cano, J. Phys. Condensed Matter **28**, 123001 (2016).
[44] C. Ederer and N. A. Spaldin, Phys. Rev. B **74**, 020401 (2006).
[45] E. Pavarini, E. Koch, and A. I. Lichtenstein, Phys. Rev. Lett. **101**, 266405 (2008).
[46] P. Wadley *et al.*, Science **351**, 587 (2016).
[47] X.-L. Li, X. Duan, Y. G. Semenov, and K. W. Kim, J. Appl. Phys. **121**, 023907 (2017).
[48] E. Bousquet, N. A. Spaldin, and K. T. Delaney, Phys. Rev. Lett. **106**, 107202 (2011).
[49] I. Dzyaloshinsky, J. Phys. Chem. Solids **4**, 241 (1958).
[50] T. Moriya, Phys. Rev. **120**, 91 (1960).
[51] B. H. Kim and B. I. Min, New J. Phys. **13**, 073034 (2011).
[52] F. Matsukura, Y. Tokura, and H. Ohno, Nat. Nanotechnol. **10**, 209 (2015).
[53] P. Borisov, A. Hochstrat, X. Chen, W. Kleemann, and C. Binek, Phys. Rev. Lett. **94**, 117203 (2005).
[54] V. Laukhin, V. Skumryev, X. Martí, D. Hrabovsky, F. Sánchez, M. V. García-Cuenca, C. Ferrater, M. Varela, U. Lüders, J. F. Bobo, and J. Fontcuberta, Phys. Rev. Lett. **97**, 227201 (2006).
[55] S. Zhou, J. Wang, X. Chang, S. Wang, B. Qian, Z. Han, Q. Xu, J. Du, P. Wang, and S. Dong, Sci. Rep. **5**, 18392 (2015).
[56] S. Zhou, J. Wang, Q. Xu, and J. Du, AIP Adv. **7**, 055827 (2017).
[57] J. F. Scott and R. Blinc, J. Phys. Condens. Matter **23**, 113202 (2011).